J Mater Sci: Mater Med (2010) 21:3049–3057
DOI 10.1007/s10856-010-4144-z

Improved mechanical long-term reliability of hip resurfacing prostheses by using silicon nitride

Wen Zhang · M. Titze · B. Cappi · D. C. Wirtz · R. Telle · H. Fischer

Received: 17 July 2009 / Accepted: 3 August 2010 / Published online: 20 August 2010

Abstract Although ceramic prostheses have been successfully used in conventional total hip arthroplasty (THA) for many decades, ceramic materials have not yet been applied for hip resurfacing (HR) surgeries. The objective of this study is to investigate the mechanical reliability of silicon nitride as a new ceramic material in HR prostheses. A finite element analysis (FEA) was performed to study the effects of two different designs of prostheses on the stress distribution in the femur–neck area. A metallic (cobalt–chromium-alloy) Birmingham hip resurfacing (BHR) prosthesis and our newly designed ceramic (silicon nitride) HR prosthesis were hereby compared. The stresses induced by physiologically loading the femur bone with an implant were calculated and compared with the corresponding stresses for the healthy, intact femur bone. Here, we found stress distributions in the femur bone with the implanted silicon nitride HR prosthesis which were similar to those of healthy, intact femur bone. The lifetime predictions showed that silicon nitride is indeed mechanically reliable and, thus, is ideal for HR prostheses. Moreover, we conclude that the FEA and corresponded post-processing can help us to evaluate a new ceramic material and a specific new implant design with respect to the mechanical reliability before clinical application.

W. Zhang (✉) · B. Cappi · R. Telle
Department of Ceramics and Refractory Materials, RWTH Aachen University, Mauerstrasse 5, 52064 Aachen, Germany
e-mail: zhangwen@ghi.rwth-aachen.de

M. Titze
Institute of General Mechanics, RWTH Aachen University, Templergraben 64, 52062 Aachen, Germany

D. C. Wirtz
Clinic of Orthopaedics and Accident Surgery, University Hospital Bonn, Bonn, Germany

H. Fischer
Department of Dental Materials and Biomaterials Research, RWTH Aachen University Hospital, Pauwelsstrasse 30, 52074 Aachen, Germany

1 Introduction

Hip resurfacing (HR) is an attractive alternative to the traditional total hip arthroplasty (THA), especially for young and active patients [1]. When compared to THA, it offers several advantages. The major advantage of HR is that it maximally conserves bone. Furthermore, easier revision, more accurate restoration of leg length, and maintenance of physiological stresses within the femur can be achieved with resurfacing hip prostheses [2–9]. Currently, Birmingham hip resurfacing (BHR) (Smith & Nephew, Memphis, TN, USA) is one of the most widely used type of HR prosthesis. The short-term and medium-term clinical results of resurfacing hip arthroplasty has been encouraging [2, 4, 6, 8, 10–12]. However, failures of hip resurfacing have also been reported [13–15]. These failures occur mainly due to femoral neck fracture and aseptic loosening [13, 16]. Unfavorable stress distribution in the femur–neck area, such as overstressing and stress shielding, can cause an increased incidence of cancellous bone fractures. Moreover, improperly performed surgical techniques can also cause the operation to fail.

Nowadays, many metal-on-metal hip resurfacing designs are marketed. Nonetheless, there is no alternative material for the HR prosthesis available yet. Compared

to the former metal-on-polyethylene and ceramic-on-polyethylene bearing pairs in hip arthroplasty, the metal-on-metal articulation has reduced the generation of wear debris leading to osteolysis and aseptic loosening of the prosthesis. Nevertheless, one cannot disregard the fact that high concentrations of cobalt and chrome in the serum and urine of patients results from the wear of modern metal-on-metal prosthesis components [1, 17–21]. Savarino et al. reported significant increase of cobalt, chromium and aluminium levels in patients with metal-on-metal total hip replacement [22]. Prospective clinical studies have shown that there is an enormous increase of cobalt and chromium ions in blood and urine levels after hip resurfacing arthroplasty [23]. Although no study has determined a safe or toxic dose of cobalt or chromium in man [24]. Hart et al. reported that the level of cobalt and chromium ions in blood are associated with the numbers of circulating lymphocytes [25]. Adverse local immune response, such as aseptic lymphocytic vasculitic-associated lesions, have been reported in association with metal-on-metal bearings [26]. In contrast, the ceramic-on-ceramic hip prostheses have been widely used regarding its excellent biocompatibility and minimum wear rate in vivo loading [27, 28]. Up to now, toxic effects have not been described within the past 40 years of THA use [29–33]. Recently, Mont, Schimmin and Ong have suggested that, ceramic articulations may be an alternative for future HR prostheses [24, 34, 35]. Cappi et al. have investigated the cytocompatibility of high strength non-oxide ceramics and suggested those materials as candidates for ceramic resurfacing hip prostheses in future [36]. Therefore, a new pair of HR components having better tribological properties is desired. Ceramic-on-ceramic articulation seems to be an apt candidate if the ceramic material is mechanically reliable under the physiological loading environment in the hip joint.

The failure of previous hip resurfacing prostheses essentially resulted from the use of inappropriate materials, poor implant design, inadequate instrumentation, and maybe improper surgical techniques. It was not, however, an inherent problem with the procedure itself [1]. With regard to the acetabular side, there have hardly been any problems related to the currently used materials and designs [17]. Finite element analysis (FEA) has been successfully used for conventional THR with ceramic head [37, 38]. Till now, according to our knowledge, no study concerned about the mechanical reliabilities of ceramic HR prostheses has been presented. As a preliminary investigation, our aim of the present study was that, through FEA and predicted lifetime data, the feasibility of using ceramic HR prostheses regarding its especially designed geometry can be determined.

2 Materials and methods

2.1 Finite element analysis

2.1.1 Finite element model

The 3D model of the femur bone was created by a 3D digital camera scanner. The proper prostheses of various designs were first generated using the software package ANSYS Workbench (version 11.0, ANSYS Inc, Canonsburg, PA). Then, the FEA was performed. For cemented prostheses, the cement mantle was assumed to have a thickness of 1.5 mm superiorly and 1 mm around the parallel sections (Fig. 1a, c). All materials were assumed to be homogeneous, isotropic, and linear elastic in the range of the applied loads that were chosen for the finite element calculations. The material properties used in the FEA models are given in Table 1. The interface between the stem from the BHR prosthesis and the patient's bone was simulated to be 'sliding' with a friction coefficient of 0.3 [39]. The interfaces between the bone and cement mantle, cement mantle and prostheses were all assumed to be perfectly 'bonded' [39]. For the remaining interfaces between the bone and prostheses, i.e., the cementless cases, we assumed 'bonded' for both the metallic and ceramic prostheses. Kaltenborn et al. [40] has reported a new surface treatment on alumina surfaces for bioactivation. Therefore, an assumption of 'bonded' interfaces in cementless cases was considered to simplify the analysis.

The geometry of our proposed ceramic HR prostheses was purpose-designed, i.e., the stemless design. Considerations of avoiding stress concentrations, which need to be carefully obeyed for designing highly loaded ceramic parts, have been taken into account. Cautious handling of those parts, both in production and in application has also been considered. Moreover, a small-diameter has been selected for the ceramic prostheses in order to maintain sufficient cup thickness so as to prevent ceramic fracture while still preserving bone [35].

In this study, ten-nodes tetrahedral finite elements were used. The intact femur bone model possessed 20,031 elements (31,552 nodes), whereas the BHR prosthesis and the newly designed stemless prosthesis each had 100,525 elements (158,326 nodes) and 92,442 elements (145,596 nodes), respectively.

2.1.2 Loading and boundary conditions

The physiological loading environment around the hip joint during normal walking was considered in this study (Fig. 1e). Here, the hip contact force and muscle forces were taken from a study of Bergmann et al. [41], and a body weight of 70 kg was assumed. Since we considered a

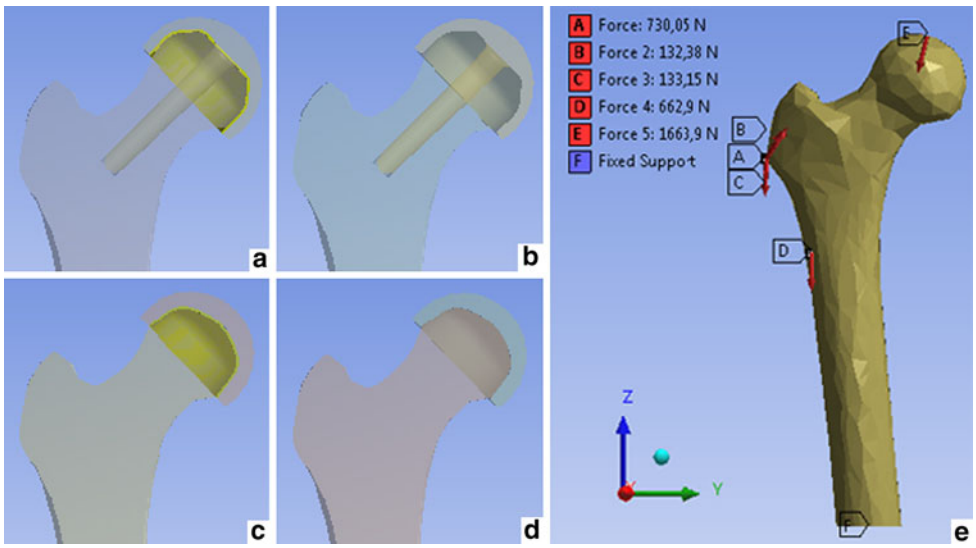

Fig. 1 Overview of the models, femur bone implanted with cemented BHR prosthesis (**a**), femur bone implanted with cementless BHR prosthesis (**b**), femur bone implanted with cemented newly designed ceramic HR prosthesis without a stem (**c**), femur bone implanted with cementless newly designed ceramic HR prosthesis (**d**), and intact femur bone model with physiological loads and boundary conditions (**e**)

Table 1 Material properties used in the FE models

	Young's modulus (GPa)	Poisson's ratio
Prosthesis (CoCr alloy)	200 [39]	0.3 [39]
Prosthesis (Si_3N_4 ceramic)	280 [56]	0.24 [56]
Cement (PMMA)	2.5 [39]	0.3 [39]
Bone	17 [55]	0.3 [55]

static analysis, the applied forces were taken from the moment when the peak load force in the hip joint was achieved during the gait. The scaled hip contact force of 1664 N was applied through the center of the femoral head. Moreover, an abductor muscle force of 729 N was applied at the greater trochanter, and a vastus lateralis muscle force of 663 N was applied at the tertius trochanter. Additionally, two other muscle forces attached to the greater trochanter were considered. The bottom of the femur shaft was fully constrained in all directions.

2.1.3 Evaluation of the FEA results

Since the femur–neck area is a critical area where femur–neck fractures usually occur, the results in this area are particularly interesting. In order to present and compare the FEA results in the femur–neck area quantitatively, a path line (Fig. 2) through the femur–neck is properly defined. The path, with a length of approx. 33 mm, starts at point A which is located in the medial superior region of the femur–neck, and ends at point B which is located in the medial inferior of the femur–neck. All the strain values along the path have been plotted in 2D diagrams according to their relative positions which allows a quantitative comparison of the results of different models. Moreover, *von Mises* strains are evaluated for the bone materials. *Von Mises* stresses and first principal stresses have been individually examined for metallic and ceramic material.

2.2 Lifetime evaluation

The fracture statistics post-processor CARES/LIFE (ceramic analysis and reliability evaluation of structure life prediction, NASA Lewis Research Center, Cleveland, OH, USA) [42, 43] was used to calculate the time-dependent reliability of the ceramic components subjected to mechanical loading. This program accounts for the phenomenon of subcritical crack growth by utilizing the power law [44]. The two-parameter Weibull cumulative distribution functions were used in the software to characterize the variation in component strength [45]. Griffith cracks were assumed to occur in our model, i.e., were chosen for the crack geometry in the model [46, 47]. Volume flaws were assumed to be responsible for ceramic failure, i.e., a volume flaw reliability analysis was performed. Theoretical long-term failure probabilities were predicted under continuous, static physiological loads for 10, 10^3, and 10^5 h, respectively. The characteristic material values used for silicon nitride were: characteristic strength, $\sigma_\Theta = 806$ MPa; Weibull modulus, $m = 9.4$. The parameters used for the subcritical crack growth in silicon nitride were: fatigue parameter, $n = 31.6$; power law constant, $B = 5.44 \times 10^5$ MPa^2 s [48].

For comparison with the silicon nitride, alumina (used for THA prostheses) has been chosen to calculate the lifetime under the same load environment. The Weibull parameters, characteristic strength, σ_Θ and Weibull modulus m of alumina (Bionit, Mathys Orthopädie, Mörsdorf, Germany) were determined in four-point bending (32 samples, stressing rate 100 MPa/s) according to German technical standards [49]. The parameters of the subcritical

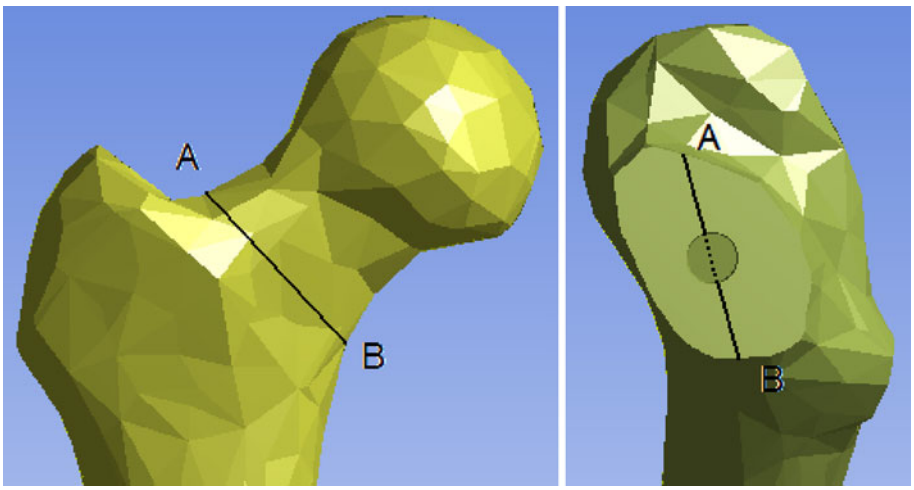

Fig. 2 Definition of the path line, points *A* and *B* represent the start and end of the defined path (*left*); cross section of the femur neck through the path line (*right*), the *vacancy* represents the removed femur bone for the accommodation of the stem, *solid line* represents the path which goes through the intact femur bone, *dashed line* represents the path which goes through the *vacancy* inside the femur bone

crack growth, n and B of this alumina material were determined using the constant stressing rate flexural strength test (ten samples for each stressing rate, stressing rates 0.1, 0.5, 1.0, and 5 MPa/s) [50]. The Weibull parameters of alumina were $\sigma_{\Theta} = 448.9$ MPa and $m = 9.1$. The subcritical crack growth parameters of alumina were $n = 37$; and $B = 3.1 \times 10^5$ MPa^2 s.

3 Results

The strain distribution in a healthy, intact femur bone is shown in Fig. 3 on the left, and the corresponding path plot is shown on the right. The highest strain value occurs at the end of the path (point B), i.e., the medial inferior region of the femur–neck. The lowest strain value appears at approx. two-thirds of the path length from point B. The strain at point A is approx. half of the value at point B. Figure 4 shows the strain distribution in femur bones implanted with BHR prosthesis, whereas Fig. 5 exhibits our newly designed ceramic prosthesis. Table 2 summarizes the strain differences between the femur bones implanted with prostheses and intact femur bones.

Compared to the intact femur bone, the BHR implant case (cemented) showed considerably greater strains of 508% at position 1/3 and of 99% at position 2/3. In addition, the cementless BHR implant case showed respectively greater strains of 438 and 305% at these corresponding positions. However, significantly better results have been found with our newly designed ceramic prosthesis when compared to the BHR cases. For cemented case, 1% overloading is predicted at point B, whereas 2 and 5% strain shielding are found at point A and position 1/3, correspondingly. For cementless case, only strain shielding of 10, 6, and 3% are predicted at point A, position 1/3 and point B, respectively. The maximum difference in strain is 5% in the cemented case and 10% in cementless case, whereby both are predicted as strain shielding.

The stress distributions in the two implants, i.e., the BHR and our new ceramic implant, were displayed in

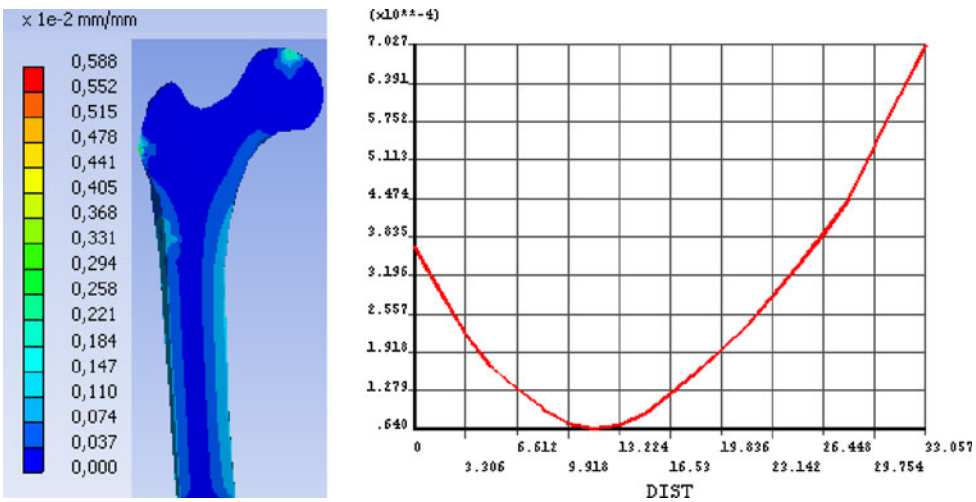

Fig. 3 *Von Mises* strain distribution in coronal cross section of the intact femur bone (*left*) and the related path plot of the strain results (*right*)

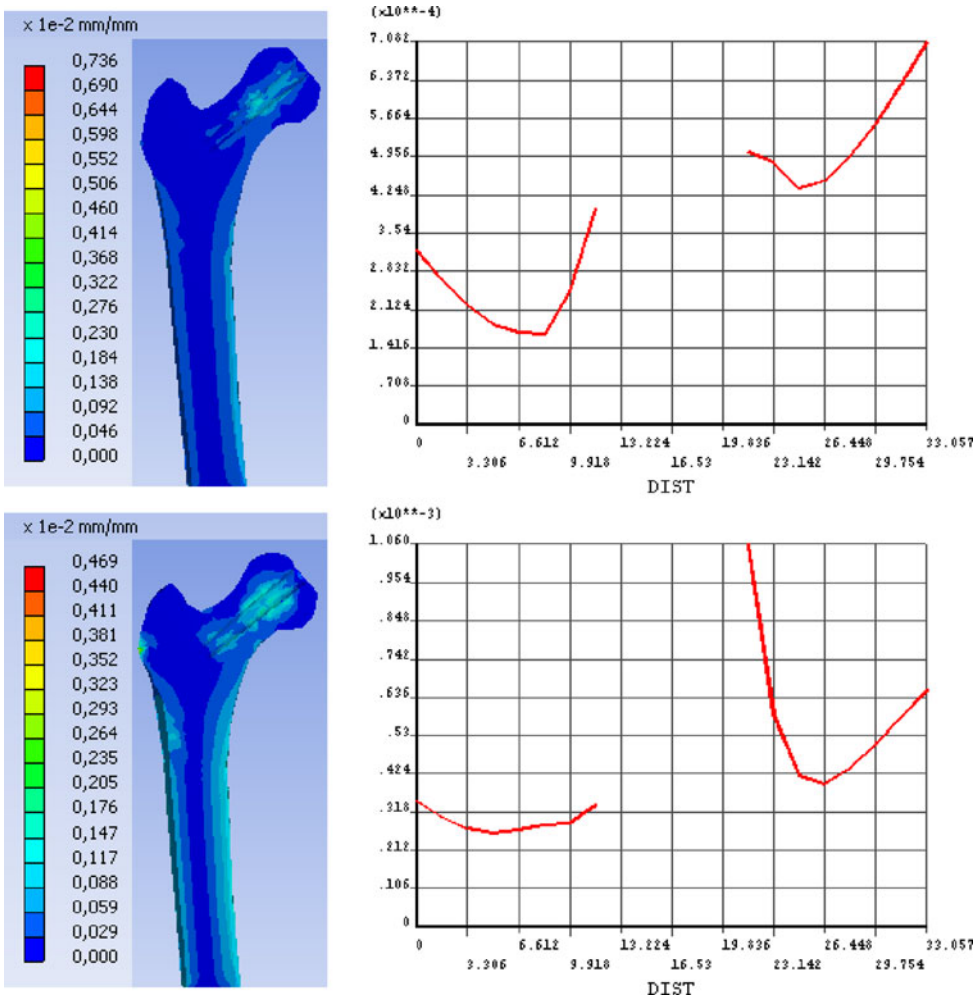

Fig. 4 *Von Mises* strain distribution in coronal cross section of the femur bones implanted with the metallic Birmingham hip resurfacing (BHR) prosthesis and the related path plots of the strain results, with cement mantle (*top*) and without cement mantle (*bottom*)

Figs. 6 and 7. The maximum *von Mises* stresses in the metallic BHR prostheses were 148 and 130 MPa for cemented and cementless cases, respectively. The maximum stress occurred inside the metallic HR prostheses underneath the loading area for the physiological hip contact force. Other stress fields were discovered around the stem of the metallic BHR prostheses for both cemented and cementless cases. Higher stress was found in the cementless case than in the cemented case. Appearing on the inside surface of the implant, the maximum first principal stresses in our newly designed ceramic HR prostheses were 28 and 36 MPa for cemented and cementless cases, respectively. Figure 8 shows the diagram of the predicted long-term failure probabilities for alumina and silicon nitride under the same loading conditions. Our analysis results revealed that alumina has failure probabilities of 0.000037% after 10 h, 0.00012% after 10^3 h (approx. 41.6 days), and 0.0004% after 10^5 h (approx. 11.4 yrs), respectively. Correspondingly, silicon nitride showed lower failure probabilities of 1.18×10^{-7}% after 10 h, 5.11×10^{-7}% after 10^3 h, and 2.20×10^{-6}% after 10^5 h.

4 Discussion

Any FEA result should be at best verified by comparing its results to experimental data. Since the experimental measurement data inside femur bones are unavailable, at present it is impossible to verify these absolute values. However, under equal loading conditions, it is possible to compare the strain results in the femur bone implanted with a prosthesis with those from a healthy, intact femur bone. Thus, to study the mechanical effects on femur bones of different implant designs, FEA results in the femur bone for each design were compared those results from the intact femur bone. All these comparisons have been summarized in Table 2. These enormous overloading may explain the frequent clinical findings of patients with femur–neck fractures several weeks after hip resurfacing surgery [13]. The role of the stem was intended to help to orient the prostheses not to take mechanical loads. However, our results imply that the stem has undertaken mechanical load and therefore, has altered the stress pattern inside the femur head. Other FEA studies [16, 39, 51, 52] also revealed

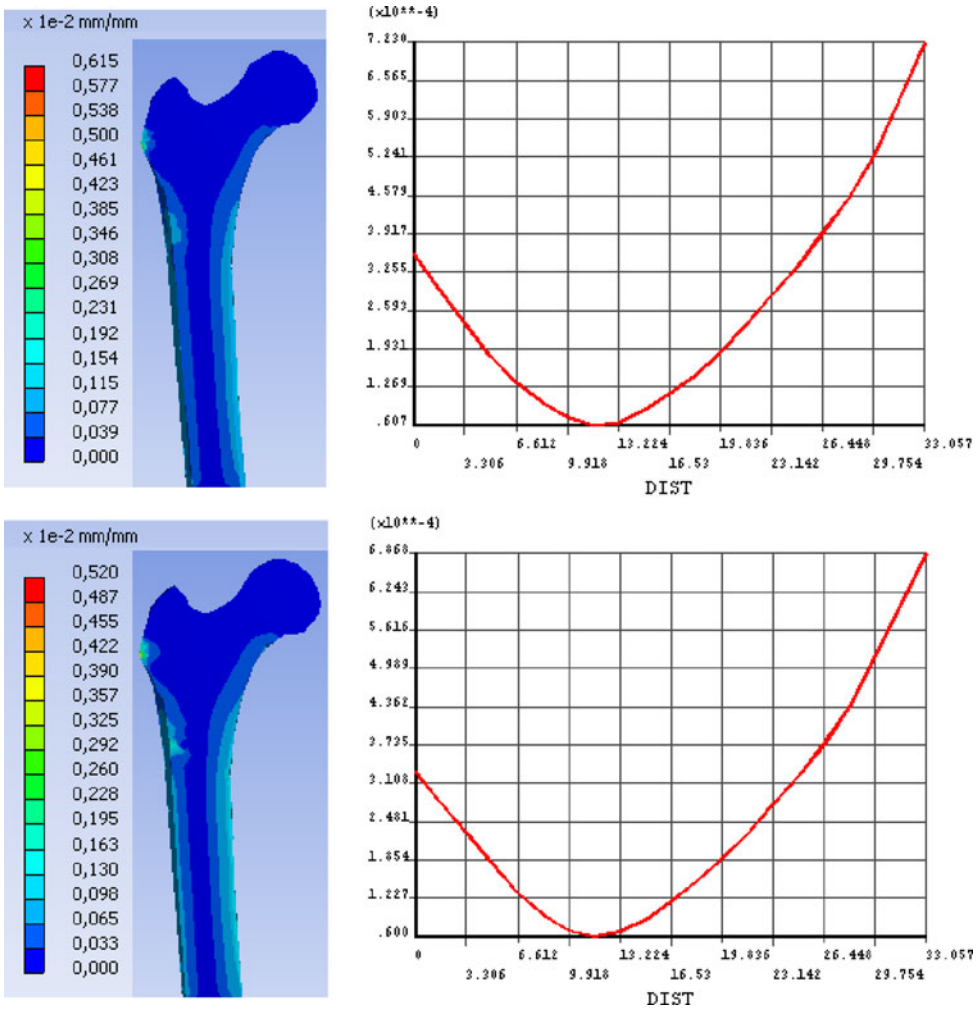

Fig. 5 *Von Mises* strain distribution in coronal cross section of the femur bones implanted with the newly designed ceramic HR prosthesis and the related path plots of the strain results, with cement mantle (*top*) and without cement mantle (*bottom*)

Table 2 Strain differences in femur bone: implanted vs. intact

	A (%)	1/3 (%)	2/3 (%)	B (%)
BHR, cemented	−14	+508	+99	+1
BHR, cementless	−1	+438	+305	−6
NDCP, cemented	−2	−5	–	+1
NDCP, cementless	−10	−6	–	−3

Differences in percentage between the femur bones implanted with prostheses and the intact femur bone

A, 1/3, 2/3, and B the four characteristic points along the path; *BHR* Birmingham hip resurfacing; *NDCP* newly designed ceramic prosthesis; '−' means strain values are lower than in intact femur bone, thus strain shielding will be predicted; '+' means strain values are higher than in intact femur bone, thus overloading will be predicted; and '–' means no comparison was made

stress fields around the stem of metallic BHR prostheses. Unphysiological loading conditions generated in the femur after implantation with a BHR prosthesis may cause later undesirable bone remodeling in the femur bone. According to this concern we introduced the new stemless design of the ceramic HR prostheses. With regard to our newly designed ceramic prosthesis, the strain differences are minimal in the cemented case. This means that the strains are almost identical to those in a healthy, intact femur bone. This indicates that our newly designed HR prosthesis bear similar physiological loads as a healthy, intact femur bone.

There is however, a concern with the simplified femur FEA model. The bone material used in the FEA models (Table 1) was assumed to be homogeneous and isotropic; no cancellous bone-like structure was hereby included. Watanabe et al. [53] and Brown et al. [54] have excluded the inhomogeneity of the bone material properties in their study. Ong et al. [35], Taylor [16] and Long et al. [51] have included the inhomogeneity of the bone material properties in their models. However, bone remodeling analyses after resurfacing were their focus, no discussions about the materials of the prostheses were made. Recently, Heijink et al. [52] studied the effect of prosthesis design on stress profile in the proximal femur after hip resurfacing. They revealed that, the stress profile of the native femur was most similar to that of the resurfaced femur with a stemless

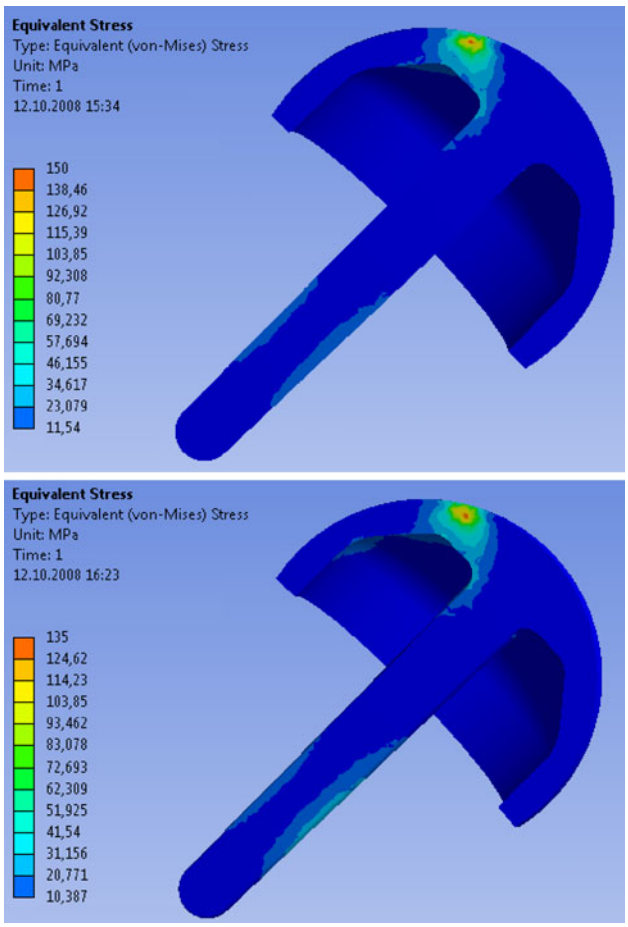

Fig. 6 *Von Mises* stress distribution in coronal cross section of the metallic BHR prosthesis, cemented (*top*) and cementless (*bottom*)

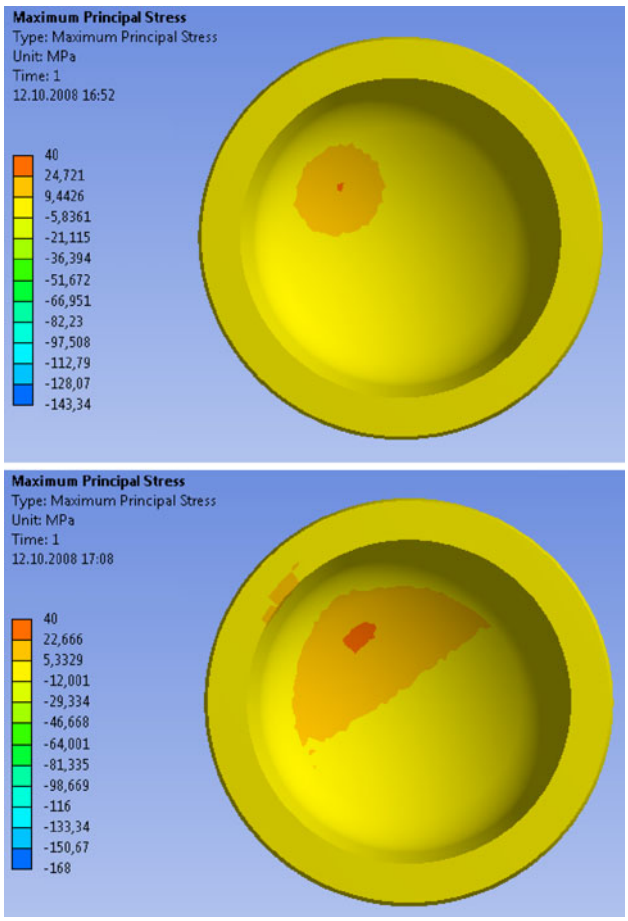

Fig. 7 First principal stress distribution in the newly designed ceramic HR prosthesis, view from bottom up, cemented (*top*), cementless (*bottom*)

prosthesis. Our results exhibited the same advantage of the newly designed stemless ceramic HR prostheses, although a simplified femur FEA model was employed in the study. Moreover, no discussions about the absolute values from the FEA were made here, rather comparisons for the different designs. Further investigations of bone remodeling in femur head resurfaced with ceramic prostheses should employ a FEA model including inhomogeneity and cancellous bone-like structure. However, as our aim was to study the mechanical feasibility of using ceramic materials in HR prostheses, prior concerns were on the mechanical examinations of ceramics. Therefore, as an elementary FEA study, the findings based on the comparisons in this study were not compromised by such a simplification.

Since alumina is the typical biocompatible ceramic used for hip replacements, we compared it with our newly proposed material silicon nitride. The long-term failure probability was evaluated, both, for alumina, and silicon nitride at constant loads under the same condition (Fig. 1e), i.e., physiological loads during normal walking. Please note, that only static loading was included in this study. Nevertheless, the lifetime predictions (Fig. 8) can help us to compare and

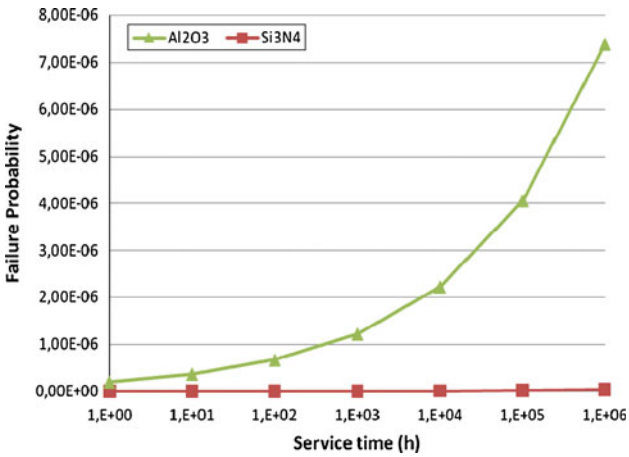

Fig. 8 Comparison of long-term failure probabilities between alumina and silicon nitride

evaluate the mechanical reliability of alumina and silicon nitride as ceramic materials for the HR prosthesis under the same boundary conditions. From a mechanical viewpoint, both alumina and silicon nitride seem to be reliable as

ceramic materials for HR prostheses. Südmeyer has drawn the conclusion that alumina is a mechanically reliable material for HR prostheses based on static FEA results [55]. In our study, silicon nitride exhibits a better mechanical behavior than alumina which is presently used in THA. This will be a benefit for implant materials in terms of an improved safety factor. However, the long-term failure probabilities may have been overestimated. The evaluations of the failure probability were performed with subcritical crack growth parameters under normal laboratory conditions (approximately 60% of relative humidity). It is known that the crack-growth parameters n and B are dependent on humidity [44]. The values of these parameters decrease with increasing humidity. Lower crack-growth values increase the subcritical crack growth and, therefore, accelerate the time-dependent reduction in strength. Thus, further in vivo or in vitro studies are necessary to verify this.

In our study, the silicon nitride exhibits potential for the ceramic HR prostheses applications, however, further investigations for its clinic use are expected. First, the FEA model of the femur should include the inhomogeneity of the bone material properties and the structure of the cancellous bone. This permits further investigation on the bone remodeling of the femur after resurfacing. Second, cyclic loads should be considered instead of static loads. Therefore, the cyclic fatigue of the ceramic HR prostheses can be analyzed. Third, a more sophisticated contact model should be integrated in order to model the press-fit interface of the ceramic HR prostheses with the bio-activated surfaces. Fourth, the in vivo measured crack-growth parameters n and B of the silicon nitride are necessary for the estimation of the long-term failure probabilities of the ceramic HR prostheses in the in vivo situation. However, as this measurement would be challenging, a straightforward substitute would be the measurement in the 100% relative humidity or in the simulated body fluid. Lastly, validations of the FEA results and the associated failure probabilities should be performed either in vitro or in vivo.

Acknowledgment We are grateful to Noel N. Nemeth, NASA, Glenn Research Center, Cleveland, OH, for supporting us with the software CARES/LIFE and for helpful discussions.

References

1. Grigoris P, Roberts P, Panousis K, Jin Z. Hip resurfacing arthroplasty: the evolution of contemporary designs. Proc Inst Mech Eng H. 2006;220:95–105.
2. McMinn D, Treacy R, Lin K, Pynsent P. Metal on metal surface replacement of the hip: experience of the McMinn prosthesis. Clin Orthop Relat Res. 1996;329(Suppl):89–98.
3. Schmalzried TP, Fowble VA, Ure KJ, Amstutz HC. Metal on metal surface replacement of the hip: technique, fixation, and early results. Clin Orthop Relat Res. 1996;329(Suppl):106–14.
4. De Smet KA, Pattyn C, Verdonk R. Early results of primary Birmingham hip resurfacing using a hybrid metal-on-metal couple. Hip Int. 2002;12:158–62.
5. Pollard TCB, Basu C, Ainsworth R, Lai W, Bannister GC. Is the Birmingham hip resurfacing worthwhile? Hip Int. 2003;13:25–8.
6. Kishida Y, Sugano N, Nishii T, Miki H, Yamaguchi K, Yoshikawa H. Preservation of the bone mineral density of the femur after surface replacement of the hip. J Bone Joint Surg Br. 2004;86:185–9.
7. Cossey AJ, Back DL, Shimmin A, Young D, Spriggins AJ. The nonoperative management of periprosthetic fractures associated with the Birmingham hip resurfacing procedure. J Arthroplast. 2005;20:358–61.
8. Treacy RB, McBryde CW, Pynsent PB. Birmingham hip resurfacing arthroplasty: a minimum follow-up of five years. J Bone Joint Surg Br. 2005;87:167–70.
9. Loughead JM, Chesney D, Holland JP, McCaskie AW. Comparison of offset in Birmingham hip resurfacing and hybrid total hip arthroplasty. J Bone Joint Surg Br. 2005;87:163–6.
10. Back DL, Dalziel R, Young D, Shimmin A. Early results of primary Birmingham hip resurfacings: an independent prospective study of the first 230 hips. J Bone Joint Surg Br. 2005;87:324–9.
11. Little CP, Ruiz AL, Harding IJ, Mclardy-Smith P, Gundle R, Murray DW, Athanasou NA. Osteonecrosis in retrieved femoral heads after failed resurfacing arthroplasty of the hip. J Bone Joint Surg Br. 2005;87:320–3.
12. De Smet KA. Belgium experience with metal-on-metal surface arthroplasty. Orthop Clin North Am. 2005;36:203–13.
13. Amstutz HC, Campbell PA, Le Duff MJ. Fracture of the neck of the femur after surface arthroplasty of the hip. J Bone Joint Surg Am. 2004;86:1874–7.
14. Shimmin AJ, Back D. Femoral neck fractures following Birmingham hip resurfacing: a national review of 50 cases. J Bone Joint Surg Br. 2005;87:463–4.
15. Shimmin AJ, Bare J, Back DL. Complications associated with hip resurfacing arthroplasty. Orthop Clin North Am. 2005;36:187–93.
16. Taylor M. Finite element analysis of the resurfaced femoral head. Proc Inst Mech Eng H. 2006;220:289–97.
17. Goebel S, Blanke M, Hendrich C. Surface replacement of the hip: contra. In: Lazennec JY, Dietrich M, editors. Ceramics in orthopaedics, 9th Biolox® symposium proceedings. Darmstadt: Steinkopff Verlag; 2004. p. 119–26.
18. Clarke MT, Lee PTH, Arora A, Villar RN. Levels of metal ions after small- and large-diameter metal-on-metal hip arthroplasty. J Bone Joint Surg Br. 2003;85:913–7.
19. Jacobs JJ, Skipor AK, Doorn PF, Campbell PA, Schmalzried TP, Black J, Amstutz HC. Cobalt and chromium concentrations in patients with metal on metal total hip replacement. Clin Orthop Relat Res. 1996;329S:256–63.
20. Jacobs JJ, Skipor AK, Patterson LM, Hallab NJ, Paprosky WG, Black J, Galante JO. Metal release in patients who have had a primary total hip arthroplasty. A prospective, controlled, longitudinal study. J Bone Joint Surg Am. 1998;80:1447–58.
21. Savarino L, Granchi D, Ciapetti G, Cenni E, Greco M, Rotini R, Veronesi CA, Baldini N, Giunti A. Ion release in stable hip arthroplasties using metal-on-metal articulating surfaces: a comparison between short- and medium-term results. J Biomed Mater Res. 2003;66A:450–6.
22. Savarino L, Greco M, Cenni E, Cavasinni L, Rotini R, Baldini N, Giunti A. Differences in ion release after ceramic-on-ceramic and metal-on-metal total hip replacement, medium-term follow-up. J Bone Joint Surg Br. 2006;88:472–6.
23. Daniel J, Ziaee H, Pradhan C, Pynsent PB, McMinn DJ. Blood and urine metal ion levels in young and active patients after

Birmingham hip resurfacing arthroplasty: four-year results of a prospective longitudinal study. J Bone Joint Surg Br. 2007;89: 169–73.
24. Mont MA, Schmalzried TP. Modern metal-on-metal hip resurfacing: important observations from the first ten years. J Bone Joint Surg Am. 2008;90:3–11.
25. Hart AJ, Skinner JA, Winship P, Faria N, Kulinskaya E, Webster D, Muirhead-Allwood S, Aldam CH, Anwar H, Powell JJ. Circulating levels of cobalt and chromium from metal-on-metal hip replacement are associated with $CD8^+$ T-cell lymphopenia. J Bone Joint Surg Br. 2009;91:835–42.
26. Willert HG, Buchhorn GH, Fayyazi A, Flury R, Windler M, Köster G, Lohmann CH. Metal-on-metal bearings and hypersensitivity in patients with artificial hip joints. A clinical and histomorphological study. J Bone Joint Surg Am. 2005;87:28–36.
27. Griss P, Werner E. Alumina ceramic, bioglass and silicon nitride. A comparative biocompatibility study. In: Hastings GW, Williams DF, editors. Mechanical properties of biomaterials. London: John Wiley & Sons Ltd; 1980. p. 217–25.
28. Willmann G. Survival rate and reliability of ceramic femoral heads for total hip arthroplasty. Mat-wiss u Werkstofftech. 1998; 29:595–604.
29. Christel PS. Biocompatibility of surgical-grade dense polycrystalline alumina. Clin Orthop Relat Res. 1992;379:10–8.
30. Dorlot JM. Long-term effects of alumina components in total hip prostheses. Clin Orthop. 1992;282:47–52.
31. Jazrawi LM, Kummer FJ, DiCesare PE. Alternative bearing surfaces for total joint arthroplasty. J Am Acad Orthop Surg. 1998;6:198–203.
32. Granchi D, Savarino L, Ciapetti G, Cenni E, Rotini R, Mieti M, Baldini N, Giunti A. Immunological changes in patients with total joint replacement following idiopathic osteoarthritis of the hip. J Bone Joint Surg Br. 2003;85:758–64.
33. Bizot P, Nizard R, Hamadouche M, Hannouche D, Sedel L. Prevention of wear and osteolysis: alumina-on-alumina bearing. Clin Orthop. 2001;393:85–93.
34. Shimmin A, Beaule PE, Campbell P. Metal-on-metal hip resurfacing arthroplasty. J Bone Joint Surg Am. 2008;90:637–54.
35. Ong KL, Manley MT, Kurtz SM. Have contemporary hip resurfacing designs reached maturity? A review. J Bone Joint Surg Am. 2008;90:81–8.
36. Cappi B, Neuss S, Salber J, Telle R, Knüchel R, Fischer H. Cytocompatibility of high strength non-oxide ceramics. J Biomed Mater Res A. 2009;93:67–76.
37. Andrisano AO, Dragoni E, Strozzi A. Axisymmetric mechanical analysis of ceramic heads for total hip replacement. Proc Inst Mech Eng H. 1990;204:157–67.
38. Prendergast PJ. Finite element models in tissue mechanics and orthopaedic implant design. Clin Biomech. 1997;12:343–66.
39. Ong KL, Kurtz SM, Manley MT, Rushton N, Mohammed NA, Field RE. Biomechanics of the Birmingham hip resurfacing arthroplasty. J Bone Joint Surg Br. 2006;88:1110–5.
40. Kaltenborn N, Sax M, Müller FA, Müller L, Dieker H, Kaiser A, Telle R, Fischer H. Coupling of phosphate on alumina surfaces for bioactivation. J Am Ceram Soc. 2007;90:1644–6.
41. Bergmann G, Deuretzbacher G, Heller M, Graichen F, Rohlmann A, Strauss J, Duda GN. Hip contact forces and gait patterns from routine activities. J Biomech. 2001;34:859–71.
42. Nemeth NN, Manderscheid JM, Gyekenyesi JP. Ceramics analysis and reliability evaluations of structures (CARES). NASA Technical Paper 2916. Cleveland: Glenn Research Centre; 1989.
43. Nemeth NN, Powers LM, Janosik LA, Gyekenyesi JP. CARES/LIFE. Users and programmers manual. Cleveland: NASA, Glenn Research Centre; 1993.
44. Munz D, Fett T. Ceramics: mechanical properties, failure behaviour, materials selection. 1st ed. Berlin: Springer; 1999.
45. Weibull W. A statistical theory of the strength of materials. Handlingar 151: Ingeniörs Vetenskaps Akademien; 1939.
46. Griffith AA. The phenomena of rupture and flaw in solids. Philos Trans R Soc. 1924;221:163–89.
47. Fischer H, Weber M, Marx R. Lifetime prediction of all-ceramic bridges by computational methods. J Dent Res. 2003;82:238–42.
48. Andrews MJ, Wereszczak AA, Breder K. Predictions of the inert strength distribution of Si_3N_4 diesel valves. Ceram Eng Sci Proc. 1999;20(3):555–63.
49. DIN EN 843-1. Advanced technical ceramics—mechanical properties of monolithic ceramics at room temperature—part 1: determination of flexural strength; 2006.
50. DIN EN 843-3. Advanced technical ceramics—mechanical properties of monolithic ceramics at room temperature—part 3: determination of subcritical crack growth parameters from constant stressing rate flexural strength tests; 2005.
51. Long JP, Santner TJ, Bartel DL. Hip resurfacing increases bone strains associated with short-term femoral neck fracture. J Orthop Res. 2009;27(10):1319–25.
52. Heijink A, Zobitz ME, Nuyts R, Morrey BF, An KN. Prosthesis design and stress profile after hip resurfacing: a finite element analysis. J Orthop Surg. 2008;16:326–32.
53. Watanabe Y, Shiba N, Matsuo S, Higuchi F, Tagawa Y, Inoue A. Biomechanical study of the resurfacing hip arthroplasty. J Arthroplast. 2000;15:505–11.
54. Brown TA, Kohan L, Ben-Nissan B. Assessment by finite element analysis of the impact of osteoporosis and osteoarthritis on hip resurfacing. 5th Australasian Congress on Applied Mechanics, ACAM 2007. Brisbane.
55. Südmeyer IJ. Dissertation: Zementfreie Hüftkopf-Oberflächenprothese aus Aluminiumoxid Orientierende FEM-Zuverlässigkeitsanalysen. Aachen: RWTH; 2008.
56. N N. Materials data silicon nitride. Germany: ESK Ceramics GmbH & Co. KG Kempten; 2006.